DESY 12-049
HU-EP-12/10
LTH 940
LPN 12-042
SFB/CPP-12-16

March 2012

On top-pair hadro-production at next-to-next-to-leading order

S. Moch[a], P. Uwer[b] and A. Vogt[c]

[a]*Deutsches Elektronensynchrotron DESY*
Platanenallee 6, D–15738 Zeuthen, Germany

[b]*Humboldt-Universität zu Berlin, Institut für Physik*
Newtonstraße 15, D-12489 Berlin, Germany

[c]*Department of Mathematical Sciences, University of Liverpool*
Liverpool L69 3BX, United Kingdom

Abstract

We study the QCD corrections at next-to-next-to-leading order (NNLO) to the cross section for the hadronic pair-production of top quarks. We present new results in the high-energy limit using the well-known framework of k_t-factorization. We combine these findings with the known threshold corrections and present improved approximate NNLO results over the full kinematic range. This approach is employed to quantify the residual theoretical uncertainty of the approximate NNLO results which amounts to about 4% for the Tevatron and 5% for the LHC cross-section predictions. Our analytic results in the high-energy limit will provide an important check on future computations of the complete NNLO cross sections.

The cross section for top-quark pair production has been measured very precisely at the hadron colliders Tevatron and LHC with an experimental accuracy challenging the precision provided by the perturbative QCD corrections at next-to-leading order (NLO), which have been known for a long time [1,2], see also [3,4]. Much recent activity has been concerned with improvements of the theoretical status beyond NLO, see [5] and refs. therein. The dominant terms at higher orders have been used to derive approximate QCD corrections to next-to-next-to-leading order (NNLO) for the inclusive cross section [6]. These consist of large threshold logarithms at next-to-next-to-leading logarithmic accuracy (NNLL) which can even be resummed to all orders in perturbation theory and could provide sufficiently precise phenomenological predictions. Yet, recent phenomenological studies based on threshold resummation to NNLL [7–11] have reported somewhat differing predictions and, moreover, have proposed different means of estimating the residual theoretical uncertainty which is predominantly due to uncalculated higher orders (beyond NNLO) and the effects of hard radiation not accounted for by threshold enhanced logarithms.

In this letter we consider the constraints on hadronic heavy-flavor production imposed by the high-energy factorization of the cross section [12, 13]. This provides important complementary information on the hard partonic scattering processes in the limit when the center-of-mass energy is much larger than the top-quark mass. It allows to extend previous approximations of the exact (yet unknown) NNLO results to the entire kinematical range and thus to obtain a more realistic uncertainty inherent in those approximate NNLO results.

The hadronic cross section for top-quark pair production is computed by the convolution of the partonic scaling functions f_{ij} with the parton luminosities $\mathcal{L}_{ij}$,

$$\sigma_{h_1 h_2 \to t\bar{t}X}(S,m) = \frac{{\alpha_s}^2}{m^2} \sum_{i,j} \int_{4m^2}^{S} ds\; \mathcal{L}_{ij}(s,S,\mu)\; f_{ij}(s,m,\mu,\alpha_s)\,, \tag{1}$$

where S denotes the hadronic center-of-mass energy squared, and m the top-quark mass in the on-shell (pole-mass) scheme. The parton luminosities $\mathcal{L}_{ij}$ are defined as

$$\mathcal{L}_{ij}(s,S,\mu) = \frac{1}{S} \int_{s}^{S} \frac{d\hat{s}}{\hat{s}} f_{i/h_1}\left(\frac{\hat{s}}{S},\mu\right) f_{j/h_2}\left(\frac{s}{\hat{s}},\mu\right)\,, \tag{2}$$

with the standard parton distribution functions (PDFs) $f_{i/h_{1,2}}(x,\mu)$. The QCD coupling constant α_s is evaluated at the scale μ in the $\overline{MS}$ scheme with n_f light flavors, and the renormalization and factorization have been identified (i.e., $\mu = \mu_r = \mu_f$). Up to NNLO, the scaling functions can be expanded as

$$f_{ij} \;=\; f_{ij}^{(0)} + 4\pi\alpha_s \left\{ f_{ij}^{(10)} + L_M f_{ij}^{(11)} \right\} + (4\pi\alpha_s)^2 \left\{ f_{ij}^{(20)} + L_M f_{ij}^{(21)} + L_M^2 f_{ij}^{(22)} \right\} + O({\alpha_s}^3)\,, \tag{3}$$

where we abbreviate $L_M = \ln(\mu^2/m^2)$. The dependence on L_M, included by the functions $f_{ij}^{(21)}$ and $f_{ij}^{(22)}$ is known exactly from [7, 14, 15].

For the high-energy factorization one considers Mellin moments ω with respect to $\rho = 4m^2/s$,

$$f_{ij}(\omega,\mu) \;=\; \int_0^1 d\rho\, \rho^{\omega-1}\, f_{ij}(\rho,\mu)\,. \tag{4}$$

The resummation of the high-energy logarithms in ρ for $\rho \to 0$, or, equivalently, of the singular terms in Mellin space as $\omega \to 0$, is based on the framework of PDFs un-integrated in the transverse momentum k_t and the concept of k_t-factorization. It is often also denoted to as small-x resummation referring to the context of deep-inelastic scattering (DIS). The procedure involves two steps, i.e., the computation of amplitudes with the initial particles off-shell in k_t, and the subsequent convolution with a gluon PDF which has the corrections for small-ρ included. For hadronic heavy-quark production, this leads to an expression for the cross section in Mellin space as a product of the (small-x resummed) gluon PDF and the corresponding impact factor depending on ω through an anomalous dimension γ_ω. which is determined by the well-known BFKL kernel.

For the purpose of this letter we are interested in the NNLO predictions of high-energy factorization in the framework of standard collinear factorization. This requires the computation of the leading terms in Mellin space as $\omega \to 0$. Using the heavy-quark impact factor of [13], the analytic result for inclusive heavy flavor hadro-production at NLO [4], the FORM routines of [16, 17], and the PSLQ algorithm as implemented in MAPLE we arrive at the following expressions for the scaling functions at high energies for a general $\mathrm{SU}(N_c)$ gauge theory, where we define $V_c = {N_c}^2 - 1$.

At Born level we have up to order $O(\omega^1)$,

$$f_{q\bar{q}}^{(0)} = \pi\Big(\frac{1}{15} - \frac{1}{15}\frac{1}{{N_c}^2}\Big) + \omega\pi\Big(-\frac{77}{450} + \frac{77}{450}\frac{1}{{N_c}^2} + \Big\{\frac{2}{15} - \frac{2}{15}\frac{1}{{N_c}^2}\Big\}\ln 2\Big)\,, \tag{5}$$

$$f_{gg}^{(0)} = \pi\Big(\frac{4}{15}\frac{N_c}{V_c} - \frac{7}{18}\frac{1}{N_c V_c}\Big) + \omega\pi\Big(-\frac{781}{900}\frac{N_c}{V_c} + \frac{43}{36}\frac{1}{N_c V_c} + \Big\{\frac{8}{15}\frac{N_c}{V_c} - \frac{7}{9}\frac{1}{N_c V_c}\Big\}\ln 2\Big)\,. \tag{6}$$

Note that subleading terms in ω, i.e.. $O(\omega^0)$ and higher are not predicted by BFKL evolution. These terms are however required for the asymptotic behavior in NNLO.

At NLO up to order $O(\omega^0)$ with n_f denoting the number of light flavors the functions read,

$$4\pi f_{q\bar{q}}^{(10)} = \frac{191}{5400}N_c - \frac{839}{8100}\frac{1}{N_c} + \frac{221}{3240}\frac{1}{{N_c}^3} - \Big\{\frac{2}{15}\frac{1}{N_c} - \frac{2}{15}\frac{1}{{N_c}^3}\Big\}\zeta_2 + \Big\{\frac{1}{50} - \frac{1}{50}\frac{1}{{N_c}^2}\Big\}n_f\,, \tag{7}$$

$$4\pi f_{q\bar{q}}^{(11)} = \frac{11}{90}N_c - \frac{11}{90}\frac{1}{N_c} - \Big\{\frac{1}{45} - \frac{1}{45}\frac{1}{{N_c}^2}\Big\}n_f\,, \tag{8}$$

$$4\pi f_{gq}^{(10)} = \frac{1}{\omega}\Big(\frac{77}{225} - \frac{41}{108}\frac{1}{{N_c}^2}\Big) - \frac{194893}{108000} + \frac{131357}{64800}\frac{1}{{N_c}^2} + \Big\{\frac{154}{225} - \frac{41}{54}\frac{1}{{N_c}^2}\Big\}\ln 2\,, \tag{9}$$

$$4\pi f_{gq}^{(11)} = \frac{1}{\omega}\Big(-\frac{2}{15} + \frac{7}{36}\frac{1}{{N_c}^2}\Big) + \frac{941}{1800} - \frac{527}{720}\frac{1}{{N_c}^2} - \Big\{\frac{4}{15} - \frac{7}{18}\frac{1}{{N_c}^2}\Big\}\ln 2\,, \tag{10}$$

$$\begin{aligned} 4\pi f_{gg}^{(10)} = {} & \frac{1}{\omega}\Big(\frac{308}{225}\frac{{N_c}^2}{V_c} - \frac{41}{27}\frac{1}{V_c}\Big) + \frac{364751}{15120}\frac{1}{V_c} - \frac{6971}{1680}\frac{1}{{N_c}^2 V_c} - \frac{736427}{108000}\frac{{N_c}^2}{V_c} \\ & + \Big\{\frac{616}{225}\frac{{N_c}^2}{V_c} - \frac{82}{27}\frac{1}{V_c}\Big\}\ln 2 + \frac{8}{15}\frac{{N_c}^2}{V_c}\zeta_2 - \Big\{\frac{11}{20}\frac{{N_c}^2}{V_c} + \frac{489}{35}\frac{1}{V_c} - \frac{141}{35}\frac{1}{{N_c}^2 V_c}\Big\}\zeta_3 \\ & + \frac{8}{9}\frac{{N_c}^2}{V_c}C_{F_4} + \frac{1}{720}\frac{N_c}{V_c}n_f\,, \end{aligned} \tag{11}$$

$$4\pi f_{gg}^{(11)} = \frac{1}{\omega}\Big(-\frac{8}{15}\frac{{N_c}^2}{V_c} + \frac{7}{9}\frac{1}{V_c}\Big) + \frac{407}{150}\frac{{N_c}^2}{V_c} - \frac{103}{27}\frac{1}{V_c} - \Big\{\frac{16}{15}\frac{{N_c}^2}{V_c} - \frac{14}{9}\frac{1}{V_c}\Big\}\ln 2\,. \tag{12}$$

Finally, at NNLO we have up to order $O(\omega^{-1})$,

$$
\begin{aligned}
(4\pi)^2 f_{q\bar{q}}^{(20)} &= \frac{1}{\omega^2}\frac{1}{\pi}\Big(\frac{2462}{3375}N_c - \frac{88463}{81000}\frac{1}{N_c} + \frac{235}{648}\frac{1}{{N_c}^3} - \Big\{\frac{1}{15}N_c + \frac{11}{360}\frac{1}{N_c} - \frac{7}{72}\frac{1}{{N_c}^3}\Big\}\zeta_2\Big) \\
&\quad + \frac{1}{\omega}C_{x,q\bar{q}}^{(20)}\,, \qquad (13) \\
(4\pi)^2 f_{q\bar{q}}^{(21)} &= \frac{1}{\omega^2}\frac{1}{\pi}\Big(-\frac{77}{225}N_c + \frac{1949}{2700}\frac{1}{N_c} - \frac{41}{108}\frac{1}{{N_c}^3}\Big) + \frac{1}{\omega}\frac{1}{\pi}\Big(\frac{222613}{108000}N_c - \frac{708437}{162000}\frac{1}{N_c} \\
&\quad + \frac{149807}{64800}\frac{1}{{N_c}^3} - \Big\{\frac{154}{225}N_c - \frac{1949}{1350}\frac{1}{N_c} + \frac{41}{54}\frac{1}{{N_c}^3}\Big\}\ln 2 - \Big\{\frac{1}{27}N_c - \frac{2}{27}\frac{1}{N_c} \\
&\quad + \frac{1}{27}\frac{1}{{N_c}^3}\Big\}n_f\Big)\,, \qquad (14) \\
(4\pi)^2 f_{q\bar{q}}^{(22)} &= \frac{1}{\omega^2}\frac{1}{\pi}\Big(\frac{1}{15}N_c - \frac{59}{360}\frac{1}{N_c} + \frac{7}{72}\frac{1}{{N_c}^3}\Big) - \frac{1}{\omega}\frac{1}{\pi}\Big(\frac{1121}{3600}N_c - \frac{2701}{3600}\frac{1}{N_c} + \frac{79}{180}\frac{1}{{N_c}^3} \\
&\quad - \Big\{\frac{2}{15}N_c - \frac{59}{180}\frac{1}{N_c} + \frac{7}{36}\frac{1}{{N_c}^3}\Big\}\ln 2\Big)\,, \qquad (15) \\
(4\pi)^2 f_{gq}^{(20)} &= \frac{1}{\omega^2}\frac{1}{\pi}\Big(\frac{2462}{1125}N_c - \frac{479}{324}\frac{1}{N_c} - \Big\{\frac{2}{15}N_c + \frac{7}{36}\frac{1}{N_c}\Big\}\zeta_2\Big) + \frac{1}{\omega}C_{x,gq}^{(20)}\,, \qquad (16) \\
(4\pi)^2 f_{gq}^{(21)} &= \frac{1}{\omega^2}\frac{1}{\pi}\Big(-\frac{77}{75}N_c + \frac{41}{36}\frac{1}{N_c}\Big) + \frac{1}{\omega}\frac{1}{\pi}\Big(\frac{1496933}{216000}N_c - \frac{3625007}{226800}\frac{1}{N_c} + \frac{6971}{3360}\frac{1}{{N_c}^3} \\
&\quad - \Big\{\frac{154}{75}N_c - \frac{41}{18}\frac{1}{N_c}\Big\}\ln 2 - \frac{4}{15}N_c\zeta_2 + \Big\{\frac{11}{40}N_c + \frac{489}{70}\frac{1}{N_c} - \frac{141}{70}\frac{1}{{N_c}^3}\Big\}\zeta_3 \\
&\quad - \frac{4}{9}N_c C_{F_4} - \Big\{\frac{293}{7200} - \frac{1}{54}\frac{1}{{N_c}^2}\Big\}n_f\Big)\,, \qquad (17) \\
(4\pi)^2 f_{gq}^{(22)} &= \frac{1}{\omega^2}\frac{1}{\pi}\Big(\frac{1}{5}N_c - \frac{7}{24}\frac{1}{N_c}\Big) + \frac{1}{\omega}\frac{1}{\pi}\Big(-\frac{1541}{1200}N_c + \frac{7871}{4320}\frac{1}{N_c} + \Big\{\frac{2}{5}N_c - \frac{7}{12}\frac{1}{N_c}\Big\}\ln 2 \\
&\quad + \Big\{\frac{1}{45} - \frac{7}{216}\frac{1}{{N_c}^2}\Big\}n_f\Big)\,, \qquad (18) \\
(4\pi)^2 f_{gg}^{(20)} &= \frac{1}{\omega^2}\frac{1}{\pi}\Big(\frac{3089}{2250}\frac{N_c}{V_c} + \frac{19696}{3375}N_c - \Big\{\frac{59}{90}\frac{N_c}{V_c} + \frac{4}{15}N_c\Big\}\zeta_2\Big) + \frac{1}{\omega}C_{x,gg}^{(20)}\,, \qquad (19) \\
(4\pi)^2 f_{gg}^{(21)} &= \frac{1}{\omega^2}\frac{1}{\pi}\Big(-\frac{616}{225}\frac{{N_c}^3}{V_c} + \frac{82}{27}\frac{N_c}{V_c}\Big) + \frac{1}{\omega}\frac{1}{\pi}\Big(\frac{358409}{18000}\frac{{N_c}^3}{V_c} - \frac{1252103}{22680}\frac{N_c}{V_c} + \frac{6971}{840}\frac{1}{N_c V_c} \\
&\quad - \Big\{\frac{1232}{225}\frac{{N_c}^3}{V_c} - \frac{164}{27}\frac{N_c}{V_c}\Big\}\ln 2 - \frac{16}{15}\frac{{N_c}^3}{V_c}\zeta_2 + \Big\{\frac{11}{10}\frac{{N_c}^3}{V_c} + \frac{978}{35}\frac{N_c}{V_c} - \frac{282}{35}\frac{1}{N_c V_c}\Big\}\zeta_3 \\
&\quad - \frac{16}{9}\frac{{N_c}^3}{V_c}C_{F_4} - \Big\{\frac{293}{1800}\frac{{N_c}^2}{V_c} - \frac{26}{75}\frac{1}{V_c} + \frac{103}{324}\frac{1}{{N_c}^2 V_c}\Big\}n_f\Big)\,, \qquad (20) \\
(4\pi)^2 f_{gg}^{(22)} &= \frac{1}{\omega^2}\frac{1}{\pi}\Big(\frac{8}{15}\frac{{N_c}^3}{V_c} - \frac{7}{9}\frac{N_c}{V_c}\Big) + \frac{1}{\omega}\frac{1}{\pi}\Big(-\frac{1771}{450}\frac{{N_c}^3}{V_c} + \frac{403}{72}\frac{N_c}{V_c} \\
&\quad + \Big\{\frac{16}{15}\frac{{N_c}^3}{V_c} - \frac{14}{9}\frac{N_c}{V_c}\Big\}\ln 2 + \Big\{\frac{4}{45}\frac{{N_c}^2}{V_c} - \frac{47}{270}\frac{1}{V_c} + \frac{7}{108}\frac{1}{{N_c}^2 V_c}\Big\}n_f\Big)\,, \qquad (21)
\end{aligned}
$$

where ζ_i denote the values of the Riemann zeta-function and the constant C_{F_4} is calculated from

$$C_{F_4} = \int_0^1 \frac{d\rho}{\rho} F_4(x) = -0.1333\,, \tag{22}$$

where $F_4(x)$ is given in eq. (19) of [4] and the value for C_{F_4} has been determined numerically.

All of the above formulae may be easily converted to momentum space with the replacements $1/\omega^2 \to -\ln\rho$ and $1/\omega \to \text{const}_\rho$, cf. eq. (4). At NNLO, the leading terms (LL_x) proportional to $1/\omega^2$ in the NNLO quantities $f_{ij}^{(2)}$ follow directly from [13]. In addition, the new next-to-leading terms (NLL_x) proportional to $1/\omega$ in the scale dependent parts $f_{ij}^{(21)}$ in $f_{ij}^{(22)}$ have been derived using standard renormalization group methods, see [7, 14, 15]. This leaves the unknown NLL_x terms denoted by $C_{x,q\bar{q}}^{(20)}$, $C_{x,gq}^{(20)}$ and $C_{x,gg}^{(20)}$ in eqs. (13), (16) and (19). It is a general feature of small-x expansions that the formally subleading terms are numerically important, and that the ratio of NLL_x to the LL_x term is large, see, e.g., eqs. (14), (17) and (20). Therefore, an estimate for these unknown terms is phenomenologically required.

We estimate $C_{x,q\bar{q}}^{(20)}$, $C_{x,gq}^{(20)}$ and $C_{x,gg}^{(20)}$ as follows. It has been observed (and also exploited constructively) [12] that the impact factors in the high energy factorization for a number of different processes with initial state hadrons are related to each other. In particular, the Abelian part of the impact factor for heavy-quark hadro-production is connected by a simple rescaling proportional to N_c from the one for heavy-quark DIS evaluated at the scale of $Q^2 = m^2$ for the photon virtuality.

In the latter case, that is for the deep-inelastic production of a heavy-quark pair via scattering off a virtual photon off an initial quark or gluon, the NLL_x terms at NNLO have recently been addressed in [18]. In DIS the heavy-quark coefficient functions are subject to an exact factorization [19] in the asymptotic limit $Q^2 \gg m^2$ into the respective coefficient functions with massless quarks and heavy-quark operator matrix elements (OMEs). The approximate NNLO results for those heavy-quark coefficient functions are based on the three-loop results of [20, 21] and can be extended to good accuracy to all scales for the photon virtuality, in particular also to the scale $Q^2 = m^2$, see [18] for details. We can use this information to estimate the ratios $r_{x,gg}$ and $r_{x,gq}$ of the NLL_x to the LL_x terms for $f_{gg}^{(20)}$ and $f_{gq}^{(20)}$ in eqs. (16), (19). Subsequently, we multiply these ratios with the exact LL_x terms of eqs. (16), (19) which assumes, of course, that the non-Abelian contributions to the NLL_x terms for heavy-quark hadro-production do not lead to significant deviations. This assumption is motivated by the fact that the LL_x terms of the scaling functions at high energy are related by simple replacements of color factors, e.g., $f_{gg}^{(10)} = 4{N_c}^2/V_c f_{gq}^{(10)}$ to LL_x accuracy. Also, in cases where the NLL_x are known exactly, e.g., the three-loop splitting functions [22], such relations still hold to a good approximation. In this way we arrive at,

$$C_{x,gq}^{(20)} = r_{x,gq}\frac{1}{\pi}\left(\frac{737813}{121500} - \frac{251}{540}\zeta_2\right) \quad \text{with} \quad r_{x,gq} = -5.6, \ldots, -7.7\,, \tag{23}$$

$$C_{x,gg}^{(20)} = r_{x,gg}\frac{1}{\pi}\left(\frac{324403}{18000} - \frac{251}{240}\zeta_2\right) \quad \text{with} \quad r_{x,gg} = -4.8, \ldots, -8.2\,, \tag{24}$$

where the terms in brackets derive from the LL_x term of eqs. (16), (19) proportional to $1/\omega^2$ with $N_c = 3$ and $V_c = 8$ substituted. The uncertainty ranges in the estimates for $r_{x,gq}$ and $r_{x,gg}$ from [18] are mainly driven by the finite number of Mellin moments currently available for the heavy-quark

OMEs [21], which limit the extrapolation to $Q^2 = m^2$. For $C_{x,gg}^{(20)}$ in eq. (24) these findings are also corroborated by the results of a Padé estimate. See e.g., [23] for definitions and the use of Padé estimates at higher orders in perturbations theory. We use eqs. (6), (11) as input for a $[0,1]$ Padé estimate of $f_{gg}^{(20)}$ to derive the value of $r_{x,gg} = -5.1$ and we have also checked that the Padé procedure predicts the NLL_x terms of $f_{gq}^{(21)}$, $f_{gq}^{(22)}$, $f_{gg}^{(21)}$ and $f_{gg}^{(22)}$ in eqs. (17), (18), (20) and (21) even with an accuracy of 5%.

For $f_{q\bar{q}}^{(20)}$ we can neither establish directly a relation to heavy-quark DIS nor can we perform a Padé estimate due to the vanishing NLO limit. Therefore, we use the same range of values for the ratio $r_{x,gg}$ given in eq. (24), however rescaled a factor 1.6 derived from the respective ratios of the NLL_x to the LL_x terms for $f_{gg}^{(0)}$ and $f_{q\bar{q}}^{(0)}$ in eqs. (5), (6). The motivation for this procedure is again, the above mentioned relations of the various scaling functions under simple exchange of color factors, see [12, 13]. Thus we use

$$C_{x,q\bar{q}}^{(20)} \;=\; r_{x,qq}\,\frac{1}{\pi}\Big(\frac{502417}{273375} - \frac{251}{1215}\zeta_2\Big) \qquad \text{with} \quad r_{x,qq} = -3.0, \ldots, -5.1\,, \tag{25}$$

where the brackets contain the LL_x result of eq. (13) with the substitution $N_c = 3$ and $V_c = 8$. As a check, we note that this procedure, if applied to the above mentioned Padé estimate for $f_{gg}^{(21)}$ and $f_{gg}^{(22)}$ predicts the NLL_x terms in $f_{q\bar{q}}^{(21)}$ and $f_{q\bar{q}}^{(22)}$ of eqs. (14), (15) again with an accuracy of typically 5%. Therefore, we conclude that the range for $r_{x,qq}$ quoted in eq. (25) is a rather conservative one.

Let us now employ the above findings. Specifically, we are interested in combining the approximations in the two kinematical regions, i.e., at threshold and at high energy (small-x) in order to arrive at smoothly interpolating functional forms for the scaling functions. Whenever possible, we compare to the exact results in order to check the quality of the approach. We choose the following ansatz for $f_{ij}^{(l)}$ at one- and two-loops,

$$f_{ij}^{(1)} \;=\; \rho^l\, f_{ij}^{(1)\mathrm{thresh}} + \beta^k\, f_{ij}^{(1)\mathrm{LL}x}\,\frac{\eta^\gamma}{C+\eta^\gamma}\,, \tag{26}$$

$$f_{ij}^{(2)} \;=\; \rho^l\, f_{ij}^{(2)\mathrm{thresh}} + \beta^k \left(-\ln\rho\, f_{ij}^{(2)\mathrm{LL}x} + f_{ij}^{(2)\mathrm{NLL}x}\,\frac{\eta^\gamma}{C+\eta^\gamma}\right), \tag{27}$$

where $\beta = \sqrt{1-\rho}$ is the heavy-quark velocity and $\eta = (1/\rho - 1)$ is the distance from threshold. For the parton channels $ij = q\bar{q}, gg$ the parameters k, l take the values $k = 3$, $l = 0$ and for $ij = gq$ we have $k = 5$, $l = 1$. These values reflect the exact functional dependence on β and ρ in the respective kinematical limits. The well-known threshold expansions are denoted $f_{ij}^{(l)\mathrm{thresh}}$ and given, e.g., in [15]. The high-energy asymptotic behavior is split in LL_x and NLL_x parts $f_{ij}^{(l)\mathrm{LL}x}$ and $f_{ij}^{(l)\mathrm{NLL}x}$ corresponding to eqs. (7)–(21). The high-η tail proportional to const_ρ (or $1/\omega$ in Mellin space) is smoothly matched with a factor $\eta^\gamma/(C+\eta^\gamma)$. The suppression parameters γ, C in eqs. (26), (27) take the following values at NLO as a best fit for $f_{ij}^{(10)}$,

$$\gamma = 0.99\,,\;\; C = 20.9 \;\text{ for } gq \qquad \text{and} \qquad \gamma = 1.18\,,\;\; C = 97.3 \;\text{ for } gg\,, \tag{28}$$

and at NNLO fitted to $f_{ij}^{(21)}$,

$$\gamma = 1.37\,,\;\; C = 47.9 \;\text{ for } q\bar{q}, \quad \gamma = 0.90\,,\;\; C = 16.4 \;\text{ for } gq \quad \text{and} \quad \gamma = 0.84\,,\;\; C = 12.6 \;\text{ for } gg\,. \tag{29}$$

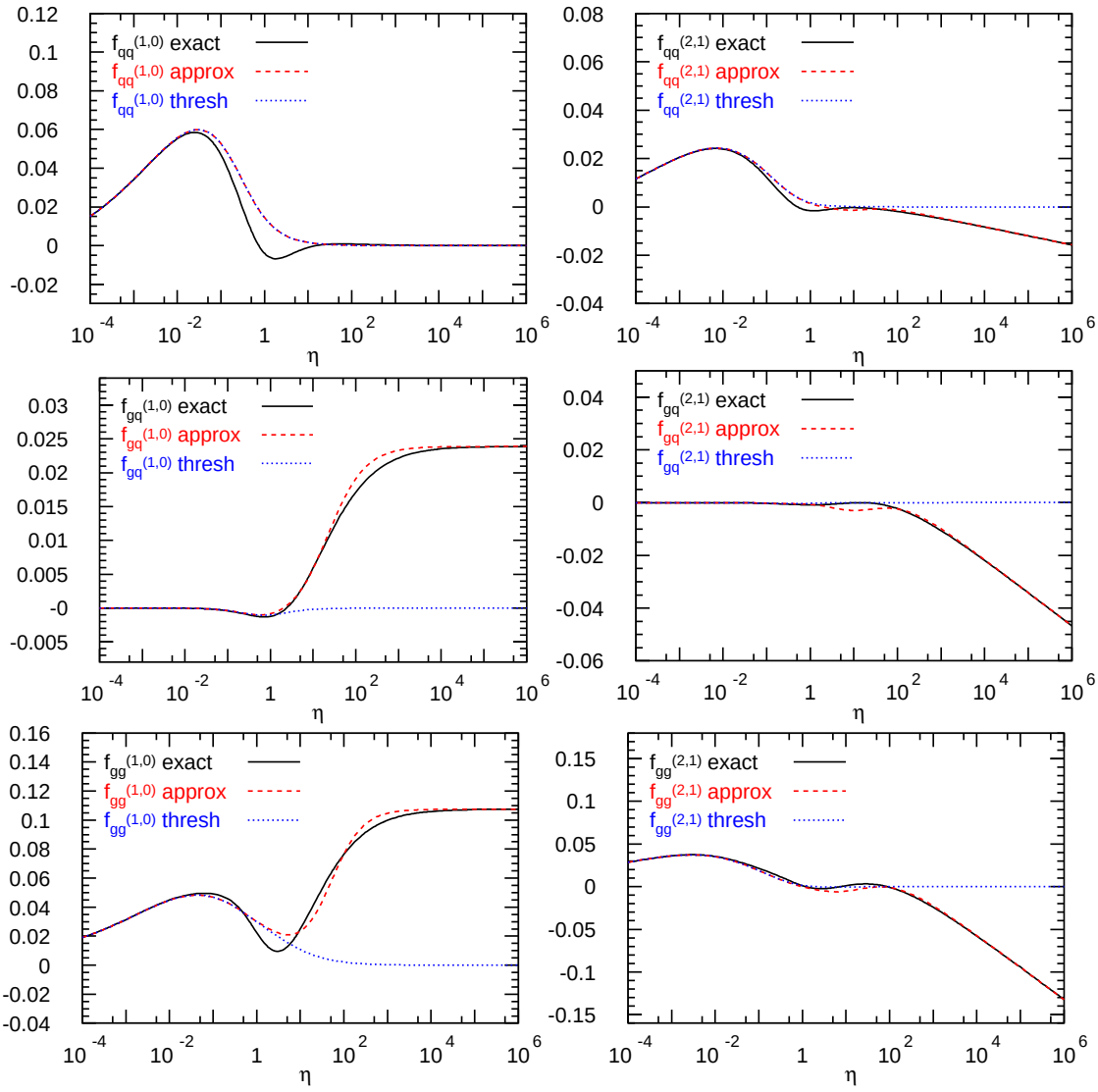

Figure 1: Comparison of exact results for $f_{ij}^{(10)}$ and $f_{ij}^{(21)}$ with the threshold expansions and the approximations defined in eqs. (26) and (27).

In Fig. 1 we show the results of this procedure for the scaling functions $f_{ij}^{(10)}$ and $f_{ij}^{(21)}$. In particular, we compare the exact results with the approximations of eqs. (26), (27) using the values of eqs. (28) and (29) for the parameters γ and C. The plots in Fig. 1 show a perfect match at both end of the kinematical range with an accuracy at the per mille level and even better as $s \to 4m^2$ and for $s \gg m^2$. This is very a strong check in particular on the results of $f_{ij}^{(21)}$ which are known numerically from renormalization group methods [7]. Some deviations between the approximations of eqs. (26), (27) and the exact results in the central range of $\eta \approx 0.1 \ldots 10$ are visible in Fig. 1. However, these have generally a small impact on cross section predictions for hadron colliders, because the necessary convolution with the parton luminosities in eq. (1) is a non-local operation and has a smoothening effect. Moreover, the parton luminosities are steeply falling functions as η grows large, giving numerically the most weight to the threshold region, which is after all the rational behind phenomenology based on the threshold resummation. In summary, the plots in Fig. 1

demonstrate that the chosen approach of combining the threshold expansion and the high-energy asymptotics leads to very good approximations of the exact scaling functions.

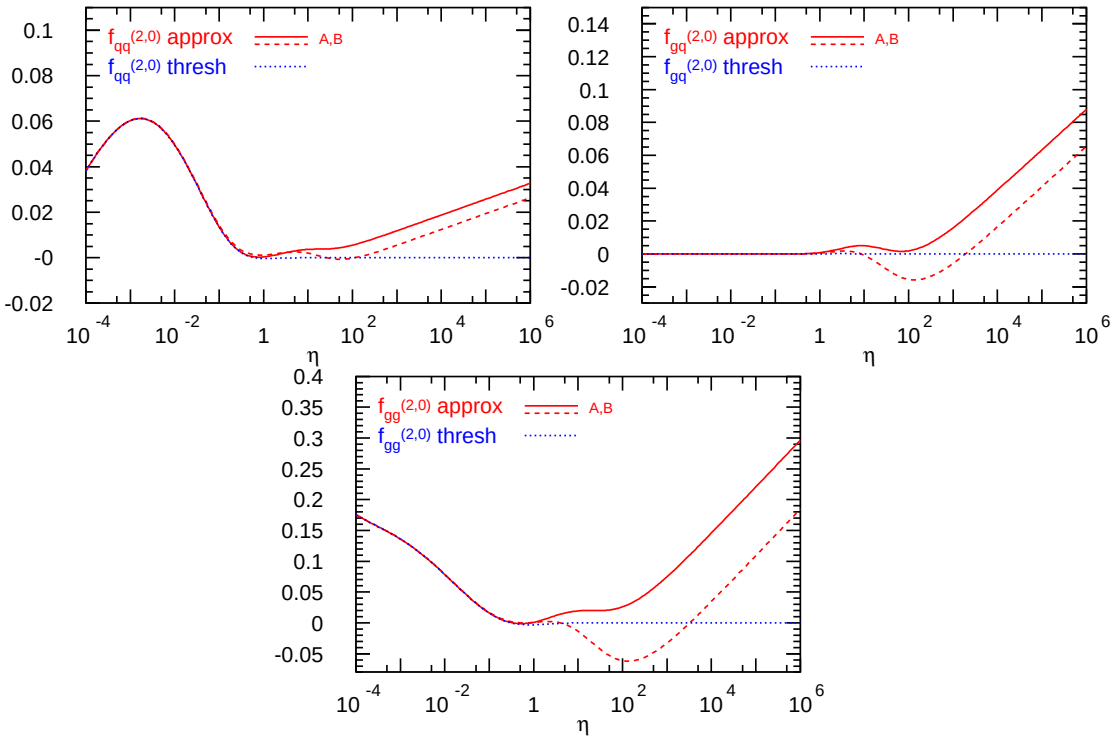

Figure 2: The threshold expansions for $f_{ij}^{(20)}$ and the approximations defined in eqs. (32) and (33). The two curves (solid=A, dashed=B) correspond to the choices for the constants given in eqs. (34)–(36).

The main object of our interest are the scaling functions $f_{ij}^{(20)}$. Here we aim at defining an uncertainty band which combines both, the threshold approximation and the high-energy limit, and also accounts for an error estimate due to the uncalculated next term in the expansions in either kinematical region. At large η, this is achieved with the NLL$_x$ terms in $f_{q\bar{q}}^{(20)}$ $f_{gq}^{(20)}$ and $f_{gg}^{(20)}$ which contain the values of $C_{x,q\bar{q}}^{(20)}$, $C_{x,gq}^{(20)}$ and $C_{x,gg}^{(20)}$ with the conservatively estimated ranges given in eqs. (23)–(25). The known threshold contributions for the functions $f_{qq}^{(20)\text{thresh}}$ and $f_{gg}^{(20)\text{thresh}}$ on the other hand contain the complete tower of logarithmically enhanced terms in $\ln^k \beta$, where $k = 1,\ldots,4$, as well as all Coulomb corrections at two loops proportional to $1/\beta^2$ and $1/\beta$ which dominate as $\beta \to 0$. Therefore, an estimate for an additional contribution of order $O(\text{const}_\beta)$ (and vanishing as $\rho \to 1$) to be added to $f_{qq}^{(20)\text{thresh}}$ and $f_{gg}^{(20)\text{thresh}}$ serves as check on their inherent uncertainty. A $[0,1]$ Padé estimate based on the exact NLO results $f_{q\bar{q}}^{(10)}$ and $f_{gg}^{(10)}$ yields for these constant $C_{\beta,q\bar{q}}^{(20)}$ and $C_{\beta,gg}^{(20)}$ in the normalization of eq. (3) the values,

$$C_{\beta,q\bar{q}}^{(20)} = \frac{f_{q\bar{q}}^{(0)}}{(4\pi)^4}\left(\frac{1276}{9} - 172\ln 2 + \frac{256}{3}\ln^2 2 - \frac{86}{3}\zeta_2 - \frac{20}{9}n_f + \frac{8}{3}n_f \ln 2\right)^2, \tag{30}$$

$$C_{\beta,gg}^{(20)} = \frac{f_{q\bar{q}}^{(0)}}{(4\pi)^4}\left(\frac{4444}{21} - \frac{2136}{7}\ln 2 + 192\ln^2 2 - \frac{283}{7}\zeta_2\right)^2, \tag{31}$$

while the default values in phenomenological studies are usually taken as $C^{(20)}_{\beta,q\bar{q}} = C^{(20)}_{\beta,gg} = 0$, see, e.g., the discussion in [15]. We neglect the gq-channel in these considerations, since it is very small near threshold anyway.

Thus, on the basis of eq. (27) and the discussion above we take the following two variants for the unknown full ρ and η dependence of the two-loop scaling functions,

$$f_{ij}^{(20)A/B} = f_{ij}^{(20)\text{thresh}} + C_{\beta,ij}^{(20)A/B} + \beta^3 f_{ij}^{(2)\text{LL}x}\left(-\ln\rho + r_{x,ij}^{A/B}\frac{\eta^\gamma}{C+\eta^\gamma}\right), \quad \text{for } ij = qq, gg, \quad (32)$$

$$f_{gq}^{(20)A/B} = \rho\, f_{gq}^{(20)\text{thresh}} + \beta^5 f_{gq}^{(2)\text{LL}x}\left(-\ln\rho + r_{x,gq}^{A/B}\frac{\eta^\gamma}{C+\eta^\gamma}\right), \quad (33)$$

where we take the same parameters γ and C for the respective channel as determined for $f_{ij}^{(21)}$ in eq. (29) and the values for $r_{x,ij}$ and $C_{\beta,ij}^{(20)}$ are chosen as

$$C_{\beta,qq}^{(20)A} = 0, \quad r_{x,qq}^{A} = -3.0, \qquad C_{\beta,qq}^{(20)B} = C_{\beta,q\bar{q}}^{(20)}, \quad r_{x,qq}^{B} = -5.1, \quad (34)$$

$$r_{x,gq}^{A} = -5.6, \qquad r_{x,gq}^{B} = -7.7, \quad (35)$$

$$C_{\beta,gg}^{(20)A} = 0, \quad r_{x,gg}^{A} = -4.8, \qquad C_{\beta,gg}^{(20)B} = C_{\beta,gg}^{(20)}, \quad r_{x,gg}^{B} = -8.2. \quad (36)$$

The results for eqs. (32) and (33) are displayed in Fig. 2. The above procedure leads to the bands shown which widen significantly for large center-of-mass energies and rise with the same slope as $s \gg m^2$ due to the known logarithmic dependence on ρ of the LL_x terms. It is evident from Fig. 2 and the numerical size of the various constants, $C_{\beta,q\bar{q}}^{(20)}$ and $C_{\beta,gg}^{(20)}$ in eqs. (30), (31) as well as $C_{x,q\bar{q}}^{(20)}$, $C_{x,gq}^{(20)}$ and $C_{x,gg}^{(20)}$ in eqs. (23)–(25) that the uncertainty in the latter is dominating even in the range of $\eta = 1\ldots100$. Therefore a more accurate determination of $C_{x,q\bar{q}}^{(20)}$, $C_{x,gq}^{(20)}$ and $C_{x,gg}^{(20)}$, preferably a computation from first principles, is highly desirable. To a minor extent, the bands in Fig. 2 depend on the chosen matching, i.e., on eq. (29). However, the values for γ and C in eq. (29) are all of the same order and, as we have shown in Fig. 1 this part of our procedure leads to reasonable descriptions in all cases where exact results are available.

	TEV $\sqrt{S} = 1.96\,\text{TeV}$	LHC $\sqrt{S} = 7\,\text{TeV}$	LHC $\sqrt{S} = 8\,\text{TeV}$	LHC $\sqrt{S} = 14\,\text{TeV}$
thresh	$6.90\,^{+0.26\ +0.16}_{-0.32\ -0.16}$	$130.4\,^{+2.9\ +5.9}_{-7.2\ -5.9}$	$190.5\,^{+3.7\ +8.0}_{-10.2\ -8.0}$	$795.3\,^{+9.0\ +23.3}_{-35.0\ -23.3}$
(A+B)/2	$7.01\,^{+0.34\ +0.16\ (+0.03)}_{-0.37\ -0.16\ (-0.03)}$	$138.5\,^{+8.1\ +6.4\ (+3.1)}_{-10.2\ -6.4\ (-3.1)}$	$202.5\,^{+11.3\ +8.6\ (+5.2)}_{-14.5\ -8.6\ (-5.2)}$	$845.5\,^{+37.3\ +25.3\ (+34.2)}_{-51.9\ -25.3\ (-34.2)}$

Table 1: The total cross section for top-quark pair-production at (approximate) NNLO using a pole mass $m = 173$ GeV and the ABM11 PDF set [24] with errors shown as $\sigma + \Delta\sigma_{\text{scale}} + \Delta\sigma_{\text{PDF}}(+\Delta\sigma_{\text{A/B}})$ The scale uncertainty $\Delta\sigma_{\text{scale}}$ is based on maximal and minimal shifts for the choices $\mu = m/2$ and $\mu = 2m$, $\Delta\sigma_{\text{PDF}}$ is the 1σ combined PDF+α_s error and the $\Delta\sigma_{\text{A/B}}$ is the deviation of the central value for either variant A or B of eqs. (32) and (33). All rates are in pb.

Let us finally investigate the implications for the total cross sections of top-quark pair-production at Tevatron and the LHC. To that end, we have implemented the approximate scaling functions

	TEV $\sqrt{S} = 1.96\,\text{TeV}$	LHC $\sqrt{S} = 7\,\text{TeV}$	LHC $\sqrt{S} = 8\,\text{TeV}$	LHC $\sqrt{S} = 14\,\text{TeV}$
thresh	$7.10\,^{+0.16\ +0.15}_{-0.14\ -0.15}$	$135.4\,^{+0.0\ +5.9}_{-3.1\ -5.9}$	$197.6\,^{+0.0\ +7.9}_{-4.9\ -7.9}$	$820.5\,^{+0.0\ +22.4}_{-24.0\ -22.4}$
(A+B)/2	$7.26\,^{+0.28\ +0.15}_{-0.20\ -0.15}\,(^{+0.04}_{-0.04})$	$146.4\,^{+4.0\ +6.5}_{-6.9\ -6.5}\,(^{+4.4}_{-4.4})$	$213.7\,^{+5.3\ +8.7}_{-9.7\ -8.7}\,(^{+7.3}_{-7.3})$	$885.7\,^{+12.3\ +25.0}_{-33.4\ -25.0}\,(^{+46.3}_{-46.3})$

Table 2: Same as Tab. 1 for a running mass $m(m) = 164$ GeV in the $\overline{MS}$ scheme.

	TEV $\sqrt{S} = 1.96\,\text{TeV}$	LHC $\sqrt{S} = 7\,\text{TeV}$	LHC $\sqrt{S} = 8\,\text{TeV}$	LHC $\sqrt{S} = 14\,\text{TeV}$
thresh	$7.13\,^{+0.30\ +0.17}_{-0.40\ -0.12}$	$164.3\,^{+3.3\ +4.4}_{-9.2\ -4.5}$	$234.6\,^{+4.1\ +5.8}_{-12.6\ -5.9}$	$908.2\,^{+9.9\ +15.2}_{-40.6\ -16.7}$
(A+B)/2	$7.27\,^{+0.41\ +0.17}_{-0.46\ -0.12}\,(^{+0.03}_{-0.03})$	$174.9\,^{+10.3\ +4.7}_{-13.2\ -4.8}\,(^{+4.6}_{-4.6})$	$249.9\,^{+14.0\ +6.2}_{-18.2\ -6.3}\,(^{+7.5}_{-7.5})$	$967.2\,^{+43.0\ +16.0}_{-60.3\ -17.6}\,(^{+44.9}_{-44.9})$

Table 3: Same as Tab. 1 for the MSTW PDF set [25].

$f_{q\bar{q}}^{(20)}$, $f_{gq}^{(20)}$ and $f_{gg}^{(20)}$ as defined in eqs. (32) and (33) in a new version of the program HATHOR [15], which otherwise uses the exact results for the scaling functions at NLO as well as for $f_{ij}^{(21)}$ and $f_{ij}^{(22)}$. Any difference that would arise from using the approximate expression eq. (27) for the scaling functions $f_{ij}^{(21)}$ instead is marginal, cf. Fig. 1.

As a central prediction we take the average of the two variants defined in eqs. (32) and (33) which we denote as '(A+B)/2' and compare to previous estimates of [7, 15] based on threshold approximation and labeled as 'thresh'. The new NNLO approximation accounts for the effect of all parton channels which are also non-zero at NLO, including the gq-channel, which picks up some contribution of the high-energy region at NNLO. However, we neglect any effect of new parton channels at NNLO, i.e., qq, $\bar{q}\bar{q}$ and $q_i\bar{q}_j$ (for unlike flavors $i \neq j$). The theoretical uncertainty is determined from the scale variation considering the choices $\mu = m/2$ and $\mu = 2m$ and taking the maximum and minimum of respective shifts of the cross sections. This is sufficient since at NNLO the μ_f dependence is generally weak and the scale uncertainty is mainly driven by the μ_r variation.

Choosing a pole mass of $m = 173$ GeV and the ABM11 PDF set [24] at NNLO our predictions are shown in Tab. 1. Comparing the threshold approximation and the new estimate '(A+B)/2' we see that there are generally small positive shifts in the cross sections due to the high-energy tail. As expected, the effect of the high-energy limit is rather modest, which nicely illustrates and confirms the stability of predictions based on soft gluon resummation. We note that the small shifts in the central values of the cross section predictions are in line with the inherent uncertainty attributed to previous approximations [7]. For the Tevatron these amount to $O(1-2\%)$ consistent with the previously observed small effect of hard radiation (not accounted for by threshold resummation) on the total cross section of $t\bar{t}$+jet production [26–28]. For the LHC at all center-of-mass energies $\sqrt{S} = 7, 8$ and 14 TeV these shifts are larger of the order $O(6-8\%)$ due to the parton luminosities $\mathcal{L}_{ij}$ giving more weight to the (positive) high-energy tail of all scaling functions in eq. (1). The scale uncertainties in the new estimate '(A+B)/2' increase compared to previous analyses – sometimes by up to a factor of two. To a large extent this increase is due to the gq-channel, where the high-energy tail is numerically more important than the threshold region, cf. Fig. 2. Taking, e.g., the values at $\sqrt{S} = 7$ TeV in Tab. 1, the cross sections split up into the contributions of the individual

channels as

$$\sigma_{(A+B)/2}(\mu = m/2) = 146.6\text{pb} = (97.4\text{pb})_{gg} + (27.9\text{pb})_{q\bar{q}} + (21.3\text{pb})_{qg}\,, \quad (37)$$

$$\sigma_{(A+B)/2}(\mu = m) = 138.5\text{pb} = (106.4\text{pb})_{gg} + (28.3\text{pb})_{q\bar{q}} + (3.8\text{pb})_{qg}\,, \quad (38)$$

$$\sigma_{(A+B)/2}(\mu = 2m) = 128.3\text{pb} = (108.5\text{pb})_{gg} + (28.5\text{pb})_{q\bar{q}} + (-8.7\text{pb})_{qg}\,. \quad (39)$$

The relatively larger impact of the qg channel can be understood from the fact that the scale dependence of its high-energy tail is not entirely compensated at the accuracy given here and, thus, leads to an increase of the scale uncertainty compared to earlier studies. This also underlines the importance of considering the high-energy regime, ignored in previous analyses [7–11], for all LHC predictions. Compared to NLO predictions however, we still observe a significant improvement. For the new estimate '(A+B)/2' we also quote the systematic uncertainty from choosing either variant A or B in eq. (32) and (33). We see for all cases that those shifts are comparable to or smaller than the scale uncertainty.

In Tab. 2 we repeat the computation for the corresponding running mass of $m = 164$ GeV in the $\overline{MS}$ scheme and similar conclusions hold with respect to the pattern of observed changes. In particular, we note that in this mass scheme better scale stability is achieved, corroborating the findings of [7]. This implies that the NNLO approximation uncertainty is considerably larger than the scale dependence for the case of LHC with $\sqrt{S} = 14\,\text{TeV}$. Finally in Tab. 3 we choose the MSTW PDF set [25] for comparison. While the Tevatron predictions of both sets are largely in agreement, the difference in the LHC predictions can be attributed to differences in the parametrization of the gluon PDFs at moderately large x and different central values for α_s, see also [24] for more PDF comparisons.

In summary we present a phenomenological study of heavy-quark hadro-production including new results in the high-energy limit as $s \gg m^2$. We have provided approximate NNLO QCD corrections for the full kinematic range based on those new constraints from high-energy factorization combined with existing results for the threshold region for $s \gtrsim 4m^2$. Our investigations have quantified the largest residual uncertainty in the two-loop scaling functions at large η due to our incomplete knowledge of the subleading 'small-x' terms in $f_{ij}^{(20)}$. In view of this it is therefore an important task to compute the exact result for those NLL$_x$ terms, $f_{ij}^{(20)}$ in eq. (27), e.g., following [12, 13] or by using the available NNLO QCD predictions for heavy-quark hadro-production in the small mass limit [29, 30]. This would immediately remove the major source of the current residual uncertainty. Other improvements of the theoretical accuracy relying on generalizations of the resummations at threshold and high-energy, e.g., along the lines of [31, 32] and [33], can be considered as well.

For the predictions of the total cross section of top-quark pair-production at Tevatron and the LHC the current available information leads to uncertainties in the approximate NNLO results which are of the order 4% for Tevatron and 5 % for the LHC. Further important corrections to be considered in phenomenological studies and not accounted for here arise from the electro-weak radiative corrections at NLO [34–36] as well as from bound state effects and the resummation of Coulomb type corrections [10, 37, 38].

At present, our approximate results represent the most complete NNLO predictions for heavy-quark hadro-production. The phenomenological importance of this process motivates further improvements to reduce the theoretical uncertainty and a number of directions for future research have been proposed. The improved QCD corrections have been implemented in a new version of

the program HATHOR [15] which is publicly available for download from [39] or from the authors upon request.

Note added:

While we were finishing this paper, numerically determined complete results for the parton channel $q\bar{q} \to t\bar{t}$ at NNLO have been presented in [40] including the double real emission $q\bar{q} \to t\bar{t}q'\bar{q}'$ for $q \neq q'$. These numerical results are not sufficient for a comparison in the high-energy region $\eta \geq 100$, where the parton channel with double real emission $q\bar{q} \to t\bar{t}q\bar{q}$ dominates. However, the results are consistent for smaller η values. Also the NNLO result of [40] is included as an option in the new version of HATHOR [15].

Acknowledgments

We thank R.K. Ellis and A. Sabio Vera for discussions. We have used the latest version of FORM [41] for the analytic calculations. This work is partially supported by the Deutsche Forschungsgemeinschaft in Sonderforschungsbereich/Transregio 9, by Helmholtz Gemeinschaft under contract VH-HA-101 (*Alliance Physics at the Terascale*), by the UK Science & Technology Facilities Council under grant number ST/G00062X/1 and by the European Commission through contract PITN-GA-2010-264564 (*LHCPhenoNet*).

References

[1] P. Nason, S. Dawson, and R. K. Ellis, Nucl. Phys. **B303**, 607 (1988).

[2] W. Beenakker, H. Kuijf, W. L. van Neerven, and J. Smith, Phys. Rev. **D40**, 54 (1989).

[3] W. Bernreuther, A. Brandenburg, Z. G. Si, and P. Uwer, Nucl. Phys. **B690**, 81 (2004), hep-ph/0403035.

[4] M. Czakon and A. Mitov, Nucl. Phys. **B824**, 111 (2010), arXiv:0811.4119.

[5] R. Bonciani and A. Ferroglia, arXiv:1201.4382.

[6] S. Moch and P. Uwer, Phys. Rev. **D78**, 034003 (2008), arXiv:0804.1476.

[7] U. Langenfeld, S. Moch, and P. Uwer, Phys.Rev. **D80**, 054009 (2009), arXiv:0906.5273.

[8] V. Ahrens *et al.*, JHEP **1009**, 097 (2010), arXiv:1003.5827.

[9] N. Kidonakis, Phys.Rev. **D82**, 114030 (2010), arXiv:1009.4935.

[10] M. Beneke, P. Falgari, S. Klein, and C. Schwinn, Nucl.Phys. **B855**, 695 (2012), arXiv:1109.1536.

[11] M. Cacciari *et al.*, arXiv:1111.5869.

[12] S. Catani, M. Ciafaloni, and F. Hautmann, Nucl.Phys. **B366**, 135 (1991).

[13] R. Ball and R. Ellis, JHEP **0105**, 053 (2001), hep-ph/0101199.

[14] N. Kidonakis, E. Laenen, S. Moch, and R. Vogt, Phys.Rev. **D64**, 114001 (2001), hep-ph/0105041.

[15] M. Aliev *et al.*, Comput.Phys.Commun. **182**, 1034 (2011), arXiv:1007.1327.

[16] J. A. M. Vermaseren, Int. J. Mod. Phys. **A14**, 2037 (1999), hep-ph/9806280.

[17] E. Remiddi and J. Vermaseren, Int.J.Mod.Phys. **A15**, 725 (2000), hep-ph/9905237.

[18] H. Kawamura, A. lo Presti, S. Moch, and A. Vogt, arXiv:1205.5727.

[19] M. Buza *et al.*, Nucl.Phys. **B472**, 611 (1996), hep-ph/9601302.

[20] J. Vermaseren, A. Vogt, and S. Moch, Nucl.Phys. **B724**, 3 (2005), hep-ph/0504242.

[21] I. Bierenbaum, J. Blümlein, and S. Klein, Nucl.Phys. **B820**, 417 (2009), arXiv:0904.3563.

[22] A. Vogt, S. Moch, and J. Vermaseren, Nucl.Phys. **B691**, 129 (2004), hep-ph/0404111.

[23] J. R. Ellis *et al.*, Phys.Rev. **D57** 2665 (1998), hep-ph/9710302.

[24] S. Alekhin, J. Blümlein, and S. Moch, arXiv:1202.2281.

[25] A. Martin, W. Stirling, R. Thorne, and G. Watt, Eur.Phys.J. **C63**, 189 (2009), arXiv:0901.0002.

[26] S. Dittmaier, P. Uwer, and S. Weinzierl, Phys. Rev. Lett. **98**, 262002 (2007), hep-ph/0703120.

[27] S. Dittmaier, P. Uwer, and S. Weinzierl, Eur. Phys. J. **C59**, 625 (2009), arXiv:0810.0452.

[28] K. Melnikov and M. Schulze, JHEP **0908**, 049 (2009), arXiv:0907.3090.

[29] M. Czakon, A. Mitov, and S. Moch, Phys. Lett. **B651**, 147 (2007), arXiv:0705.1975.

[30] M. Czakon, A. Mitov, and S. Moch, Nucl. Phys. **B798**, 210 (2008), arXiv:0707.4139.

[31] S. Moch and A. Vogt, JHEP **0911**, 099 (2009), arXiv:0909.2124.

[32] G. Soar, S. Moch, J. Vermaseren, and A. Vogt, Nucl.Phys. **B832**, 152 (2010), arXiv:0912.0369.

[33] A. Vogt, JHEP **1110**, 025 (2011), arXiv:1108.2993.

[34] W. Beenakker *et al.*, Nucl. Phys. **B411**, 343 (1994).

[35] W. Bernreuther, M. Fücker, and Z.-G. Si, Phys. Rev. **D74**, 113005 (2006), hep-ph/0610334.

[36] J. H. Kühn, A. Scharf, and P. Uwer, Eur. Phys. J. **C51**, 37 (2007), hep-ph/0610335.

[37] K. Hagiwara, Y. Sumino, and H. Yokoya, Phys. Lett. **B666**, 71 (2008), arXiv:0804.1014.

[38] Y. Kiyo *et al.*, Eur. Phys. J. **C60**, 375 (2009), arXiv:0812.0919.

[39] Hathor, `http://www.physik.hu-berlin.de/pep/tools/` or `http://www-zeuthen.desy.de/~moch/hathor` .

[40] P. Bärnreuther, M. Czakon and A. Mitov, arXiv:1204.5201.

[41] J. Vermaseren, arXiv:math-ph/0010025.